PCCP

PAPER

View Article Online
View Journal | View Issue

Cite this: *Phys. Chem. Chem. Phys.*, 2015, **17**, 20830

Determining adsorbate configuration on alumina surfaces with ^{13}C nuclear magnetic resonance relaxation time analysis

P. A. Vecino,[a] Z. Huang,[a] J. Mitchell,*[b] J. McGregor,†[a] H. Daly,[c] C. Hardacre,[c] J. M. Thomson[c] and L. F. Gladden[a]

Received 27th April 2015,
Accepted 21st July 2015

DOI: 10.1039/c5cp02436f

www.rsc.org/pccp

Relative strengths of surface interaction for individual carbon atoms in acyclic and cyclic hydrocarbons adsorbed on alumina surfaces are determined using chemically resolved ^{13}C nuclear magnetic resonance (NMR) T_1 relaxation times. The ratio of relaxation times for the adsorbed atoms $T_{1,ads}$ to the bulk liquid relaxation time $T_{1,bulk}$ provides an indication of the mobility of the atom. Hence a low $T_{1,ads}/T_{1,bulk}$ ratio indicates a stronger surface interaction. The carbon atoms associated with unsaturated bonds in the molecules are seen to exhibit a larger reduction in T_1 on adsorption relative to the aliphatic carbons, consistent with adsorption occurring through the carbon–carbon multiple bonds. The relaxation data are interpreted in terms of proximity of individual carbon atoms to the alumina surface and adsorption conformations are inferred. Furthermore, variations of interaction strength and molecular configuration have been explored as a function of adsorbate coverage, temperature, surface pre-treatment, and in the presence of co-adsorbates. This relaxation time analysis is appropriate for studying the behaviour of hydrocarbons adsorbed on a wide range of catalyst support and supported-metal catalyst surfaces, and offers the potential to explore such systems under realistic operating conditions when multiple chemical components are present at the surface.

1 Introduction

The adsorption of molecules onto active surface sites is a fundamental step in heterogeneous catalysis. To develop an improved understanding of catalytic reaction mechanisms on a molecular level it is necessary to identify the configuration adopted by molecules upon adsorption, the nature of the surface interaction, and the strength of this interaction. For instance, the geometry occupied by reactant molecules is critical in dictating both their activity and reaction kinetics, while the efficacy of chiral modifiers is known to be dependent upon their conformation on a catalyst surface.[1] Many techniques applied both under high vacuum and at realistic process conditions have been employed previously to probe the interaction of adsorbates with catalyst surfaces.[2,3] There remains, however, a lack of information on the molecular configuration of molecular species at interfaces.[4]

Nuclear magnetic resonance (NMR) techniques offer the potential for probing adsorbate–adsorbent interactions. Previous studies have focused on the change in the chemical shift δ of the NMR spectral line associated with an atom that occurs on adsorption. When a chemical species is adsorbed, the distribution of electrons within the molecule is distorted, altering the degree of chemical shielding experienced by the nucleus. A larger chemical shift change $\Delta\delta$ indicates stronger adsorption.[5] This interpretation can be complicated by external factors such as the change of polarisation within an adsorbed molecule[6] and the variation with surface coverage.[7] Nevertheless, this method has been used to study the chemisorption of hydrogen on Pt and Pd surfaces using ^1H NMR,[7] and of fluorine-containing adsorbates on a variety of surfaces, including aluminas, using ^{19}F NMR.[8] ^{13}C NMR has been used to investigate oligomers grafted onto silica surfaces,[9] ionic surfactants adsorbed on silica,[5] and in applications to catalysis; for example, hydrocarbon adsorption on zeolites.[6] The use of ^{13}C NMR has practical advantages over ^1H NMR. Significant line broadening of the spectral resonances occurs for adsorbed species as a result of differences in magnetic susceptibility at the liquid–solid interface. This line broadening can prevent the identification of individual ^1H

[a] *Department of Chemical Engineering and Biotechnology, University of Cambridge, Pembroke Street, Cambridge CB2 3RA, UK*
[b] *Schlumberger Gould Research, High Cross, Madingley Road, Cambridge CB3 0EL, UK. E-mail: JMitchell16@slb.com*
[c] *School of Chemistry and Chemical Engineering, Queen's University, Belfast, BT9 5AG, UK*
† Present address: Department of Chemical and Biological Engineering, The University of Sheffield, Sir Robert Hadfield Building, Mappin Street, Sheffield S1 3JD, UK.

resonances due to the limited chemical shift range associated with the ^{1}H nucleus. In contrast, the much larger chemical shift range of ^{13}C means that it is possible to distinguish the individual resonances even for the broadened lines of adsorbed molecules,[10] hence the surface interaction of each individual carbon atom in an adsorbed hydrocarbon can be examined.

An alternative NMR probe of surface interaction is the longitudinal relaxation time T_1. The nuclear spin relaxation behaviour of a chemical species adsorbed onto a surface is modified by the strength of that interaction.[11–13] The molecular motion (translation and rotation) of the adsorbate on the adsorbent surface is described by the autocorrelation function $G(\tau)$ averaged over the time interval τ. The Fourier-transform of this function is proportional to the longitudinal relaxation time T_1. The autocorrelation function of the molecule will change on adsorption, and hence a change in T_1 is observed. In general, energetically stable adsorption conformations (corresponding to reduced mobility of the surface-bound species) are associated with stronger surface interactions. The ratio of T_1 relaxation times for surface adsorbed to free diffusing (bulk) molecules $T_{1,ads}/T_{1,bulk}$ can therefore be used as an indicator of the relative strength of surface interaction assuming the motional narrowing regime applies always, such that $\omega_0\tau \ll 1$, where ω_0 is the Larmor frequency. A low $T_{1,ads}/T_{1,bulk}$ ratio is associated with low mobility and hence stronger adsorption.

Previously, we have used the ratio of longitudinal to transverse relaxation times T_1/T_2 to probe the relative strengths of interaction between chemical species in liquid saturated porous catalysts using two-dimensional ^{1}H relaxometry techniques.[14] In a fully saturated porous medium, this ratio of relaxation times is preferable as it removes the influence of pore geometry that would be significant in, say, the $T_{1,pore}/T_{1,bulk}$ ratio. Here, we do not need concern ourselves with the geometric effects because we are probing only a monolayer on the pore surface and as such can directly compare the relaxation time of the adsorbed liquid molecules to those in the bulk. Also, the use of T_2 relaxation time measurements is suboptimal in these high-field NMR experiments because the magnetic susceptibility differences between the solid, and the adsorbed liquid and vapour phases may prevent accurate interpretation of the results;[15] it is established that T_1 relaxation times are independent of such artefacts.[16]

The inference of adsorption properties from NMR relaxation parameters has been investigated previously by Monduzzi *et al.* with regard to the interaction of cyclic molecules, including pyrrole, with the surface of zeolites.[13] It was observed that the C3 carbon atoms of pyrrole (*i.e.* those furthest from the nitrogen heteroatom) had a shorter $T_{1,ads}$ relaxation time than the C2 carbon atoms. This was explained as a loss of mobility for the C3 carbons due to their involvement in the solid–liquid interaction. Molecular modelling calculations confirmed that the species binding to the surface through the C3 carbons represented the most energetically stable configuration. Elsewhere, Popova and co-workers have employed ^{13}C NMR in order to investigate the variation in T_1 along the carbon-chain of a surfactant inside porous SiO_2.[5] In this case the pore space was filled with liquid surfactant and hence the adsorbate–adsorbent interaction was not probed directly; it was modified by molecular exchange with bulk liquid in the pore. As neither of these studies considered the ratio of the measured relaxation time against that of the bulk liquid, only general trends could be established. It is important to consider a ratio, as different carbon atoms within a molecule can have different T_1 values in the bulk phase and it is the variation of T_1 on adsorption that reveals the relative strength of surface interaction.

To date, ^{13}C T_1 measurements of adsorbed species have not, to the best of our knowledge, been exploited as a tool for comparing the relative surface interaction strengths of each carbon in an adsorbed hydrocarbon molecule and hence used as an indicator for adsorbate configuration. We have inferred information previously on the relative strength of adsorbate–adsorbent interactions from two-dimensional ^{1}H relaxation analysis (without chemical shift information) in catalytic systems.[14] Here, we demonstrate the use of chemical shift resolved ^{13}C NMR T_1 measurements to probe the adsorption of individual carbon atoms within their parent molecules. These measurements are straightforward to conduct and analyse, and yield direct information on the molecular configuration and relative adsorption strength of adsorbate molecules; the technique is described in Section 2. In Section 3.1 we present a study of the adsorption of a series of acyclic C_5 and cyclic C_6 hydrocarbons on θ-Al_2O_3 and γ-Al_2O_3. Acyclic C_5 molecules provide a proxy for molecules of interest in many industrially-relevant catalysed reactions, such as hydrogenation or isomerisation.[17] Cyclic C_6 species are important as intermediates in the processing of petrochemical feedstocks.[18] These NMR data are supported by conventional Diffuse Reflectance Infrared Fourier-Transform Spectroscopy (DRIFTS) results. The influences of surface coverage, surface pre-treatment, and temperature on the geometry of adsorbed hydrocarbons are explored in Section 3.2. To highlight the versatility of the NMR technique, we explore the conformation of 1-pentene when co-adsorbed with carbon monoxide and other hydrocarbons (see Section 3.3). It is not possible to characterise the surface geometry of co-adsorbed species using conventional techniques such as DRIFTS. The presence of a co-adsorbate allows us to consider how the interaction of the alkene with the active surface sites might be modified during a catalytic reaction where products and solvents will be present alongside the reactant. Two cases are considered; the solid phase used is θ-Al_2O_3 in both cases. First, we consider the co-adsorption of species representative of those relevant to industrially catalytic processes of interest. In particular, the co-adsorption of CO or 2-butyne is considered. The co-adsorption of CO with 1-pentene has been selected because of its relevance to the industrial semi-hydrogenation of acetylene where CO is added as a co-adsorbate to improve selectivity.[19] The co-adsorption of 1-pentene and 2-butyne allows us to explore the relative strength of triple-bond and double-bond interactions. In both cases, two experiments are performed. In the first experiment, 1-pentene is pre-adsorbed prior to admitting the CO or 2-butyne to the system. In the second experiment, the order of adsorption is reversed, with 1-pentene adsorption occurring after adsorption of CO or 2-butyne. The second case considered was

the adsorption of 1-pentene following adsorption of cyclohexane or benzene; these cyclic species were chosen as models for soft and hard coke, respectively.

2 Materials and methods

Both θ-Al_2O_3 (Johnson Matthey, BET surface area 120 $m^2\ g^{-1}$, BJH pore volume 0.57 $cm^3\ g^{-1}$) and γ-Al_2O_3 (Johnson Matthey, BET surface area 190 $m^2\ g^{-1}$, BJH pore volume 0.70 $cm^3\ g^{-1}$) were supplied as trilobe extrudates of approximate dimensions 10 mm × 1 mm (length × width). The adsorbates studied include a series of acyclic C_5 hydrocarbons (of purity): 1-pentene (98%), 1-pentyne (99%), *cis*-2-pentene (98%), *trans*-2-pentene (99%), and 1,4-pentadiene (99%). For reference, the bond structures and carbon numbers are portrayed for each of these molecules in Fig. 1(a–e). Additional studies were conducted on a series of unsaturated cyclic C_6 hydrocarbons (of purity): cyclohexene (99%), 1,4-cyclohexadiene (97%), and 1,3-cyclohexadiene (97%); the bond structures and carbon numbers of these cyclic molecules are represented in Fig. 1(f–h). Benzene (99%), 2-butyne (99%), and cyclohexane (99%) were used in the co-adsorption studies. All the hydrocarbons were obtained from Sigma-Aldrich at the stated purities. CO (99%, <5 ppm H_2O, Air Liquide) was used without further purification.

For the NMR relaxation time measurements of the adsorbates in the adsorbed state, $T_{1,ads}$, the hydrocarbons were adsorbed onto the aluminas *via* a glass vacuum line (Soham Scientific Ltd). A glass basket containing 3.5 g of Al_2O_3 trilobes was attached to the vacuum line and evacuated to a pressure $<10^{-2}$ mbar. The liquid hydrocarbon was degassed *via* several freeze–evacuate–thaw cycles and admitted to the vacuum line in the gas-phase at a known pressure. The sample basket was cooled using liquid nitrogen to condense the hydrocarbon onto the alumina surface.

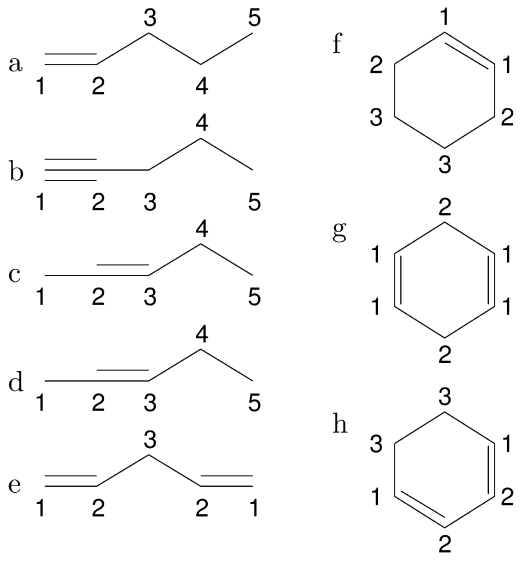

Fig. 1 Structure and carbon numbers of (a) 1-pentene, (b) 1-pentyne, (c) *cis*-2-pentene, (d) *trans*-2-pentene, (e) 1,4-pentadiene, (f) cyclohexene, (g) 1,4-cyclohexadiene, and (h) 1,3-cyclohexadiene. Carbons are numbered according to independent ^{13}C NMR resonances.

Adsorption was confirmed by a corresponding reduction in pressure in the vacuum line. The basket was then flame-sealed. This process was repeated for each of the C_5 and C_6 hydrocarbons on both θ-Al_2O_3 and γ-Al_2O_3. Surface coverages were calculated assuming a uniform distribution of the hydrocarbon, estimating the surface area occupied by an individual molecule from the excluded molecular area of *n*-pentane (4.2×10^{-19} m^2) for the C_5 adsorbates and 2-butyne, and cyclohexane (4.7×10^{-19} m^2) for the C_6 adsorbates and benzene.[20] For example, 3.5 g of γ-Al_2O_3 has a total surface area of 665 m^2 and can therefore accommodate 1.58×10^{21} molecules of *n*-pentane, equivalent to 2.6×10^{-3} moles. Therefore, in order to obtain a theoretical coverage approximating but not exceeding 1 monolayer (ML), approximately 2×10^{-3} moles of the C_5 species were introduced into the alumina trilobes. NMR measurements were also performed on individual liquid species in order to obtain the $T_{1,bulk}$ values. For these studies, the hydrocarbons were dosed into empty glass baskets as received. Co-adsorption experiments were performed with 1-pentene on θ-Al_2O_3. For cyclohexane and benzene, adsorption of 0.5 ML of 1-pentene was performed after 0.9 ML of the co-adsorbate was dosed on the alumina. In the case of 1 pentene and CO, and 1-pentene and 2-butyne, 0.5 ML of 1-pentene was adsorbed, followed by 0.5 ML of the co-adsorbate, and *vice-versa*. A $T_{1,bulk}$ relaxation time for CO in the gas phase could not be determined due to the low ^{13}C density at atmospheric pressure. Consequently, the $T_{1,ads}/T_{1,bulk}$ ratio of physisorbed CO was not obtained.

The NMR experiments were performed on a Bruker DMX spectrometer with a vertical bore 7 T superconducting magnet. The radio frequency (r.f.) excitation and detection was achieved using a birdcage resonator tuned to 75 MHz for ^{13}C. T_1 relaxation properties of both bulk liquid and adsorbed hydrocarbons were measured using the standard inversion-recovery pulse sequence, with signal acquired in the presence of ^1H broadband decoupling. T_1 values were determined by fitting a single-component exponential recovery function to the data. Due to the limited homogeneity of the applied r.f. magnetic field, it was necessary to acquire the ^{13}C spectral information in two separate experiments spanning chemical shift ranges of 0–100 ppm and 100–200 ppm. The experiments were performed at 20 °C, unless reported otherwise; bulk and surface relaxation times were compared at the same temperature in all cases. The spectra were referenced to the ^{13}C resonance of tetramethylsilane (TMS). The errors associated with fitting the bulk $T_{1,bulk}$ relaxation times were all within ±2%, whilst the errors associated with fitting the adsorbed $T_{1,ads}$ relaxation times were all within ±5%. Therefore, the total errors on the $T_{1,ads}/T_{1,bulk}$ ratios are considered to be less than ±7%. The measurements with 1-pentene were repeated several times on fresh samples and found to be consistent. The repeat data fell within the errors quoted here. The theoretical foundation which enables us to correlate $T_{1,ads}/T_{1,bulk}$ with adsorption strength has been discussed in detail elsewhere.[12,21]

DRIFTS measurements were acquired for the adsorption of 1-pentene over θ-Al_2O_3 and γ-Al_2O_3 powders. The alumina trilobes were crushed in order to prepare the sample as a powder.

Adsorption of the alkene over KBr was also performed to provide a reference spectrum for the 1-pentene on a non-adsorbing surface. All spectra were recorded at 4 cm^{-1} resolution, using a Bruker Equinox 55 spectrometer equipped with an MCT detector. The alumina samples were treated *in situ* to partially dehydroxylate the surface, prior to adsorption of the alkene. This treatment consisted of heating to 500 °C with a 10% O_2 in Ar atmosphere flowing at 100 ml min^{-1}, holding for 1 hour at 500 °C, and then cooling to 35 °C under Ar flow. The 1-pentene was then adsorbed onto the alumina at 35 °C. Once the alumina surface was saturated (detected by no further change in the spectra) the feed was switched to Ar at 20 ml min^{-1} and desorption of the alkene was monitored. During desorption, spectra were recorded every 15 s.

3 Results and discussion

3.1 Conformation of adsorbed hydrocarbons

3.1.1 Acyclic hydrocarbons. The measured $T_{1,ads}/T_{1,bulk}$ ratios for the individual carbon atoms within acyclic C5 species adsorbed on θ-Al_2O_3 and γ-Al_2O_3 are shown in Fig. 2. In all cases, the $T_{1,ads}/T_{1,bulk}$ ratios associated with olefinic or acetylinic carbons, *i.e.*, those atoms linked by unsaturated carbon–carbon double or triple bonds, are consistently lower than the $T_{1,ads}/T_{1,bulk}$ ratios associated with the aliphatic carbons (those linked by a saturated carbon–carbon single bond) in the same molecule. Considering *cis*-2-pentene on θ-Al_2O_3, Fig. 2(c) (squares), as a typical example, the olefinic C2 and C3 carbons exhibit $T_{1,ads}/T_{1,bulk}$ ratios of 0.048 and 0.043, respectively. These values are lower than for the aliphatic (C1, C4 and C5) carbon atoms where $T_{1,ads}/T_{1,bulk}$ ratios of 0.109, 0.065, and 0.133 are observed, respectively. The $T_{1,bulk}$ relaxation times are determined by intra- and inter-molecular interactions, and so are partly dependent on the flexibility of the carbon backbone. By taking the ratio $T_{1,ads}/T_{1,bulk}$ for each carbon atom, we account for the influence of this bulk relaxation mechanism and so are sensitive to changes in flexibility on adsorption, as well as the usual enhanced relaxation due to nuclear spin interactions with the surface. Therefore, it is concluded that the olefinic carbon atoms experience a relatively stronger interaction with the alumina surface than the aliphatic carbons. The terminal aliphatic carbon (C5) shows the weakest interaction. These data suggest that for *cis*-2-pentene, and indeed all the acyclic molecules studied, adsorption occurs primarily through the unsaturated carbon–carbon multiple bonds as expected. Although previous studies have observed the existence of a di-σ bond between alkenes and metal surfaces,[22,23] only a weak molecular interaction was observed between the adsorbate and the alumina surface for the systems studied here, as confirmed by DRIFTS studies, see Fig. 3 and discussion below. A di-σ bond would also result in the loss of the olefinic lines from the ^{13}C NMR spectrum due to the change in the electron distribution and hence degree of chemical shielding on the ^{13}C nucleus; loss of the olefinic resonances is not observed.

Comparing an alkene (1-pentene, Fig. 2(a)) and an alkyne (1-pentyne, Fig. 2(b)), we see a more pronounced difference between the $T_{1,ads}/T_{1,bulk}$ ratios of the acetylenic and aliphatic

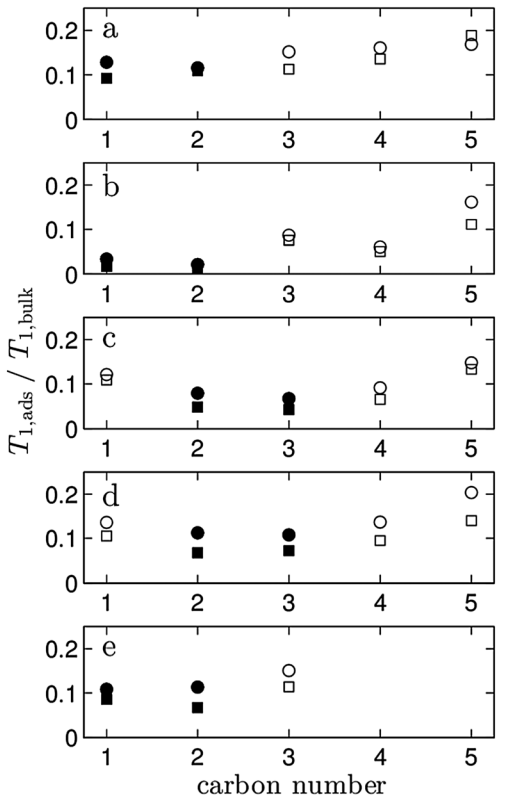

Fig. 2 The ratio of surface to bulk relaxation times $T_{1,ads}/T_{1,bulk}$ for the individual carbon atoms in (a) 1-pentene, (b) 1-pentyne, (c) *cis*-2-pentene, (d) *trans*-2-pentene, and (e) 1,4-pentadiene adsorbed on θ-Al_2O_3 (squares) and γ-Al_2O_3 (circles). The carbon numbers correspond to the schematic diagrams in Fig. 1. Solid symbols represent olefinic or acetylinic carbons associated with the unsaturated carbon–carbon bonds, and open symbols represent aliphatic carbons.

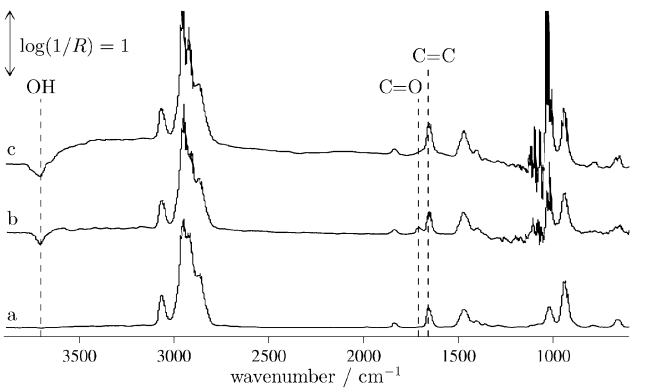

Fig. 3 DRIFTS of 1-pentene adsorbed over (a) KBr, (b) θ-Al_2O_3, and (c) γ-Al_2O_3 at 35 °C. There is no significant change in band position with surface and the ν(C=C) band is observed at 1647 cm^{-1} in all cases. The loss of ν(OH) bands is observed on both alumina surfaces following adsorption of 1-pentene which together with the lack of perturbation of the C=C band suggests relatively weak adsorption. The ν(C=O) band observed at 1705 cm^{-1} over θ-Al_2O_3 may be attributable to partial oxidation of the 1-pentene. Spectra are displayed as log(1/*R*), where *R* is the ratio of the relative reflectance of a surface with 1-pentene adsorbed to the relative reflectance of a cleaned surface.

carbons in the alkyne than between the olefinic and aliphatic carbons in the alkene. This variation corresponds to the greater adsorption strength of alkynes through the carbon–carbon triple bond compared to alkenes through the carbon–carbon double bond, as has been established previously.[24]

The observed $T_{1,ads}/T_{1,bulk}$ ratios are lower, consistently, for species adsorbed on θ-Al_2O_3, Fig. 2 (squares), than on γ-Al_2O_3, Fig. 2 (circles). This result implies stronger adsorption on θ-Al_2O_3, as expected from the higher surface Lewis[25] and Brønsted[26] acidities of θ-Al_2O_3 compared to γ-Al_2O_3. However, it is important to note that, for a given molecule, the same general trends in $T_{1,ads}/T_{1,bulk}$ ratio are seen on both surfaces when compared on an atom-by-atom basis. Therefore, the type of interaction and molecular configuration adopted upon adsorption is similar on the two forms of alumina.

The use of ^{13}C NMR to study individual carbon atoms allows additional information to be obtained. Notably, the geometry occupied by the adsorbate on the adsorbent surface can be considered. Since T_1 is associated with the strength of interaction of an atom with the adsorbent surface, it can also be used as a qualitative indicator of the distance between the atom and the surface. Again considering *cis*-2-pentene as a representative example, the olefinic C2 and C3 carbons have the greatest surface interaction and so are assumed to be located closer to the surface than the aliphatic carbon atoms. The different $T_{1,ads}/T_{1,bulk}$ ratios of C1 and C4 suggests the molecule does not adsorb in a planar (symmetric) fashion around the double-bond. This interpretation is consistent with the molecular configuration proposed for alkene adsorption on catalytically-relevant surfaces from other spectroscopic studies.[4,23,27] Buchbinder and co-workers employed broadband vibrational sum-frequency generation spectroscopy (SFG) to study the adsorption of molecules including 1-pentene and *cis*-2-pentene on an α-Al_2O_3 (0001) surface.[4] The results reported in this paper are consistent with the conclusions from SFG spectroscopy. However, the latter does not provide information on individual carbon atoms but rather explores the behaviour of functional groups, *e.g.*, methyl or methylene functionalities. Analysis of the NMR data can yield additional information, is more straightforward to interpret and is not dependent upon selection rules that render vibrations in particular planes undetectable. Furthermore, the NMR experiments are conducted over adsorbates in an industrially relevant physical form, while a single crystal surface has to be employed as the adsorption surface in the SFG studies.

Molecular conformations are inferred assuming adsorption on a flat surface. However, the measurements are actually giving us an average measurement of the interaction strength of each carbon atom with the surface – whether that surface is or is not flat. Thus, given that the surface of the real alumina surface is unlikely to be either energetically or physically 'flat', and that the observed $T_{1,ads}$ times are weighted heavily by the strongest surface adsorption sites, the measurements provide us with the ability to identify differences in average adsorbate configuration between different adsorbates and different substrates in real materials. The sensitivity of the measurement to the strongest interaction sites between adsorbate and solid surface is an advantage in understanding the role that differences in adsorption configuration play in subsequent catalytic behaviour.

The data for 1,4-pentadiene are shown in Fig. 2(e). The symmetric nature of the molecule means that only three distinct carbon resonances are observed in the bulk liquid. On adsorption, a single $T_{1,ads}$ relaxation time was observed for the aliphatic carbons, consistent with the molecule adsorbing symmetrically. If the olefinic carbons adsorbed to different extents, a two-component relaxation time for one or both of the $T_{1,ads}$ values for the C1 and C2 carbons would be observed.

In addition to NMR relaxation time analysis, the adsorption of 1-pentene adsorbed on KBr, θ-Al_2O_3 and γ-Al_2O_3 was investigated by DRIFTS studies. Comparison of the spectra of 1-pentene over the KBr and the alumina surfaces in Fig. 3 shows no significant change in position or relative intensity of the 1-pentene bands. The loss of OH groups from the alumina surfaces (indicated by negative bands in Fig. 3) suggests that the alkene interacts with the OH groups *via* H-bonds.[28,29] The ν(C=C) band is present at 1641 cm^{-1} over all the surfaces indicating that there is no perturbation of the C=C bond following adsorption. This observation is consistent with the relaxation time data in Fig. 2 which suggests that the olefinic carbons interact more strongly than the aliphatic carbons with the surface, with C1 and C2 having a very similar interaction strength. DRIFTS was used to follow desorption of 1-pentene from the saturated surface. Bands due to 1-pentene were no longer observed after approximately 10 minutes for desorption from γ-Al_2O_3, whereas on θ-Al_2O_3, the ν(C=C) band was still detectable after 20 minutes. These data support the $T_{1,ads}/T_{1,bulk}$ analysis that suggest that 1-pentene adsorbs more strongly on θ-Al_2O_3 than γ-Al_2O_3.

3.1.2 Cyclic hydrocarbons. Fig. 4 shows the $T_{1,ads}/T_{1,bulk}$ ratios for cyclohexene, 1,4-cyclohexadiene, and 1,3-cyclohexadiene adsorbed on θ-Al_2O_3 and γ-Al_2O_3. In each case, only three distinct resonances are observed in the NMR spectra as a result of molecular symmetry. The single $T_{1,ads}$ times associated with each resonance line indicate that the equivalent carbon atoms experience similar interactions with the surface.

A stronger interaction is observed for the adsorbed olefinic carbons than for the aliphatic carbons in the cyclic hydrocarbons. There is no indication in the NMR spectra of the C_6 hydrocarbons that the double-bonds break, suggesting that adsorption occurs again *via* a weak interaction with surface OH groups. A more detailed examination of the relative strength of interaction of each carbon in a given molecule allows adsorption conformations to be proposed. For many cyclic molecules, a number of different adsorption geometries are theoretically possible and experimental evidence is required to determine which conformation exists on a given surface. Considering 1,4-cyclohexadiene adsorption on θ-Al_2O_3, the data are consistent with a boat conformation where the C1 carbons are in close proximity to the surface whilst the C2 carbons are slightly further from the surface. In a similar manner, the data for adsorbed cyclohexene suggest a di-σ boat conformation. The implied geometries of all three cyclic C_6 species are consistent with conclusions reported previously as a result of

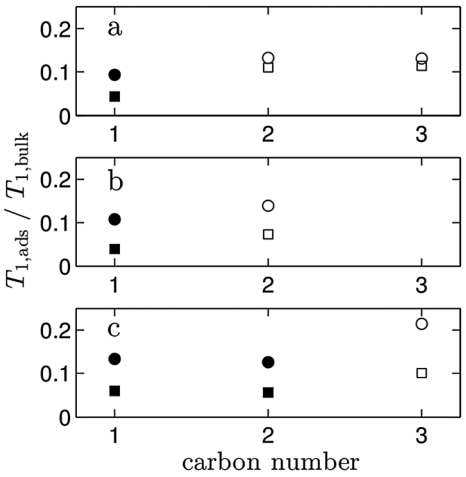

Fig. 4 The ratio of surface to bulk relaxation times $T_{1,ads}/T_{1,bulk}$ for the individual carbon atoms in (a) cyclohexene, (b) 1,4-cyclohexadiene, and (c) 1,3-cyclohexadiene adsorbed on θ-Al_2O_3 (squares) and γ-Al_2O_3 (circles). The carbon numbers correspond to the schematic diagrams in Fig. 1. Solid symbols represent olefinic carbons associated with the unsaturated carbon–carbon double bonds, and open symbols represent aliphatic carbons.

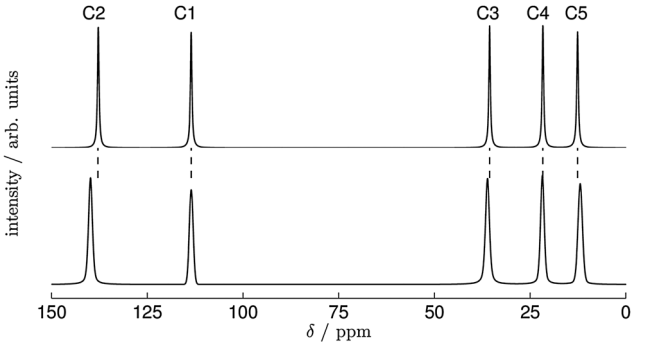

Fig. 5 ^{13}C spectra for 1-pentene (top) as bulk liquid and (bottom) adsorbed on θ-Al_2O_3. The dashed lines correspond to the position of the resonance lines in the bulk liquid to indicate the change in chemical shift that occurs on adsorption.

experimental surface science and theoretical investigations on Pt(111)[3,30]

In a comparison of Fig. 2 and 4, similar $T_{1,ads}/T_{1,bulk}$ ratios are obtained in the acyclic and cyclic compounds. For example, the olefinic carbons in cyclohexene adsorbed on θ-Al_2O_3 exhibit $T_{1,ads}/T_{1,bulk}$ = 0.044, comparable to an average $T_{1,ads}/T_{1,bulk}$ = 0.046 for the olefinic carbons in *cis*-2-pentene. Similarly, the aliphatic carbons in cyclohexene on θ-Al_2O_3 have an average $T_{1,ads}/T_{1,bulk}$ = 0.112, comparable to an average $T_{1,ads}/T_{1,bulk}$ = 0.102 for the aliphatic carbons in *cis*-2-pentene. These data suggest that the bonding mechanisms, and relative strengths of the bonds, are similar for both types of organic molecule.

3.1.3 Comparison of relaxation time and chemical shift. Surface adsorption has been probed previously by observing the change in chemical shift $\Delta\delta$ that occurs when a molecule bonds with a surface. Given the line broadening that occurs when a liquid is adsorbed onto a heterogeneous surface, due primarily to the difference in magnetic susceptibilities between the adsorbent and adsorbate, obtaining accurate chemical shift information in these samples can be difficult. Notwithstanding, a $\Delta\delta$ per atom for the acyclic C_5 molecules adsorbed on both the θ-Al_2O_3 and γ-Al_2O_3 surfaces was estimated. An example of the chemical spectrum (post-processed with a peak fitting algorithm) obtained for 1-pentene adsorbed on θ-Al_2O_3 is shown in Fig. 5; the bulk liquid spectrum is included for comparison. The aliphatic carbons have the smallest chemical shifts whereas the olefinic carbons have larger chemical shifts. It is interesting to note that the C1 and C4 carbon atoms exhibit almost no change in chemical shift on adsorption, even though C1 is associated with the olefinic bond and hence is expected to interact with the alumina surface *via* its bonding electrons. The resonance corresponding to C2 is shifted downfield by $\Delta\delta$ = 3 ppm; this relatively small shift is consistent with a weak interaction of the double-bond with surface Brønsted acid sites.[31] C3 has a smaller shift of $\Delta\delta < 1$ ppm. The terminal carbon C5 exhibits an upfield shift of $\Delta\delta = -1$ ppm. The same trends in $\Delta\delta$ have been noted previously in ^{13}C NMR studies of alkane adsorption on zeolites.[6]

Thus, while significant information on the nature of adsorption can be revealed through measurements of $\Delta\delta$, we suggest that the use of atom-specific $T_{1,ads}/T_{1,bulk}$ ratios provides a more detailed and less ambiguous description of the surface interaction. For instance, no change in δ is observed (suggesting negligible surface interaction) for the olefinic C1 carbon in 1-pentene (Fig. 5), whereas the $T_{1,ads}/T_{1,bulk}$ ratio indicates a stronger interaction of the C1 carbon with the alumina surface compared to the aliphatic carbons (Fig. 2(a)), as expected. In general, changes in chemical shift upon adsorption do correlate with adsorption strength but the change in δ, unlike the relaxation time analysis which is sensitive only to molecular mobility, will be determined by the change in electronic configuration introduced by the adsorption interaction of the nucleus of interest which results in a modification to the chemical shielding effects around that nucleus. If that change in electron distribution is influenced by factors other than the adsorption interaction, a direct correlation between $\Delta\delta$ and adsorption strength will not hold. Further, the much broader linewidths associated with the nuclei of molecules in the adsorbed state introduces additional uncertainties in the precise value of $\Delta\delta$ characterising a given system. Overall, we conclude that $T_{1,ads}/T_{1,bulk}$ offers a more direct indication of the surface interaction strength than $\Delta\delta$ in these systems.

3.2 Influence of physical factors on the conformation of adsorbed hydrocarbons

3.2.1 Surface coverage. The results reported in Section 3.1.1 described the adsorption of acyclic species with approximately 1 ML of surface coverage. In order to investigate the influence of surface coverage on molecular configuration, the adsorption of 1-pentene on θ-Al_2O_3 has been further investigated at approximately 0.5 ML and 0.2 ML. Fig. 6 shows the $T_{1,ads}/T_{1,bulk}$ ratios determined for these samples. It appears that the overall strength of adsorption of 1-pentene decreases

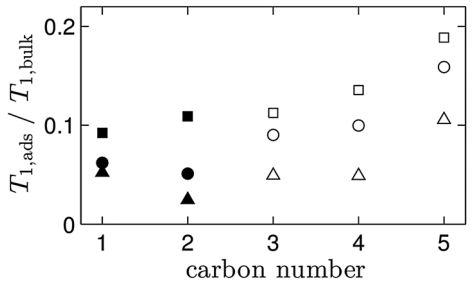

Fig. 6 The ratio of surface to bulk relaxation times $T_{1,ads}/T_{1,bulk}$ for the individual carbon atoms in 1-pentene adsorbed on θ-Al_2O_3 with a surface coverage of approximately 1 ML (squares), 0.5 ML (circles), and 0.2 ML (triangles). Solid symbols represent olefinic carbons and open symbols represent aliphatic carbons.

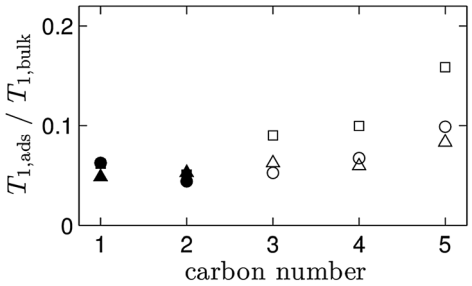

Fig. 7 The ratio of surface to bulk relaxation times $T_{1,ads}/T_{1,bulk}$ for the individual carbon atoms in 1-pentene adsorbed on θ-Al_2O_3 with a surface coverage of 0.5 ML at 20 °C (squares), 10 °C (circles), and 0 °C (triangles). Solid symbols represent olefinic carbons and open symbols represent aliphatic carbons.

with increasing surface coverage. Consider, for instance, the C3 carbon where the $T_{1,ads}/T_{1,bulk}$ ratio changes from 0.049 at 0.2 ML to 0.113 at 1 ML. The surface of θ-Al_2O_3 is heterogeneous in nature with a number of different adsorption sites available including Lewis acid (Al^{3+}) and Brønsted acid (OH) sites.[32] Both the NMR chemical shift and DRIFTS data suggest that the dominant interaction is *via* the Brønsted acid sites. It is expected that the strongest adsorption sites are populated initially, followed by weaker sites. As the coverage increases, it is reasonable to assume that the average strength of the adsorption decreases as the alkene molecules are forced to occupy surface sites in which they experience a weaker surface interaction. An additional factor may be the disruption of the alkene–alumina interaction through steric effects on approaching saturation of the surface.[33] Also, the average $T_{1,ads}$ for a given molecule may exhibit some dependence on surface coverage due to variations in intermolecular spin interactions. Note, however, that there is a significant increase in the $T_{1,ads}/T_{1,bulk}$ ratio of the C2 carbon atom as coverage increases. A much smaller change is observed for C1 in Fig. 6. This observation indicates that the nature of the interaction of the carbon–carbon double bond with the adsorbent surface is coverage dependent. TPD studies have indicated decreasing energy of interaction with increasing surface coverage in the adsorption of similar alkenes.[34]

3.2.2 Temperature. Similarly to the effect of coverage upon adsorption of 1-pentene on θ-Al_2O_3, it is relevant to determine the effect of temperature on interaction strength and geometry of adsorption. Additional measurements were therefore performed on 0.5 ML 1-pentene adsorbed on θ-Al_2O_3 at two additional temperatures: 0 °C and 10 °C. Fig. 7 shows the NMR relaxometry results of 0.5 ML 1-pentene on θ-Al_2O_3 at all temperatures studied. An increase in surface interaction is observed with decreasing temperature. The interaction of the olefinic carbons C1 and C2 are insensitive to temperature. The aliphatic carbons C3–C5 are sensitive to temperature with a notable decrease in the interaction of the C3, C4 and C5 carbons with the surface in raising the temperature from 10 to 20 °C. The most significant change was observed for the terminal carbon (C5), where $T_{1,ads}/T_{1,bulk}$ = 0.159 at 20 °C decreased to $T_{1,ads}/T_{1,bulk}$ = 0.099 at 10 °C, and then to $T_{1,ads}/T_{1,bulk}$ = 0.084 at 0 °C.

The results in Fig. 7 indicate that 1-pentene adsorption *via* the double-bond is negligibly affected by temperature in the range 0–20 °C. The interaction of the alkyl chain with the surface is very similar at 0 and 10 °C, but a significant decrease in interaction with the surface is observed in increasing the temperature from 10 to 20 °C. These results imply a decrease in the alkyl chain mobility with decreasing temperature, consistent with an increase in lateral molecule–molecule interactions, as observed during adsorption of propane–propylene mixtures.[35]

3.2.3 Surface pre-treatment. The effect of pre-treatment temperature on alumina surfaces has been widely reported in the literature to have a significant effect on acid site density and the Brønsted to Lewis acid site ratio.[29,36] It is therefore expected that adsorption of hydrocarbons on alumina will be influenced by pre-treatment temperature. Adsorption of 0.5 ML of 1-pentene was carried out on θ-Al_2O_3 following pre-treatment of the θ-Al_2O_3 by heating to 400 °C at a rate of 20 °C min^{-1} and then held for 2 h under vacuum. The $T_{1,ads}/T_{1,bulk}$ data are shown in Fig. 8. In addition to 1-pentene, NMR spectral analysis revealed the presence of *trans*-2-pentene at a molar ratio of 1 : 2 *trans*-2-pentene to 1-pentene. Here, strong adsorption of both molecules is implied by the $T_{1,ads}/T_{1,bulk}$ ratios. In 1-pentene, C2 exhibits the strongest surface interaction with $T_{1,ads}/T_{1,bulk}$ = 0.002. This value contrasts with $T_{1,ads}/T_{1,bulk}$ = 0.051 observed for C2 on θ-Al_2O_3 pre-treated at room temperature, Fig. 2(a). The olefinic region of 1-pentene has an average $T_{1,ads}/T_{1,bulk}$ ratio of 0.006 when the alumina is pre-treated at 400 °C, and 0.056 when the alumina is prepared at room temperature. Similarly for the aliphatic chain we observe average $T_{1,ads}/T_{1,bulk}$ ratios of 0.018 on alumina pre-treated at 400 °C and 0.116 on alumina prepared at room temperature. Therefore, a considerably stronger interaction is implied when 1-pentene is adsorbed on pre-heated alumina. Pre-treatment of the alumina at high temperatures results in the removal of hydroxyl groups. The corresponding increase in Lewis acid site density at the higher temperature[37] explains the stronger interaction of 1-pentene through the carbon–carbon double bond. Modification of the Lewis acid site density by the pre-treatment process permits isomerisation of 1-pentene to *trans*-2-pentene (no *cis*-2-pentene was detected). Isomerisation of *n*-butene to 2-butenes

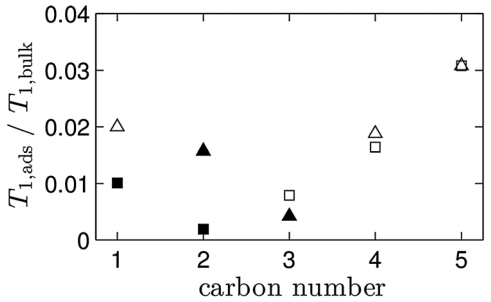

Fig. 8 The ratio of surface to bulk relaxation times $T_{1,ads}/T_{1,bulk}$ for the individual carbon atoms observed on pre-heated θ-Al_2O_3 at 400 °C after the adsorption of 0.5 ML 1-pentene. 1-Pentene (squares) and *trans*-2-pentene (triangles) were identified by chemical shift. Solid symbols represent olefinic carbons and open symbols represent aliphatic carbons.

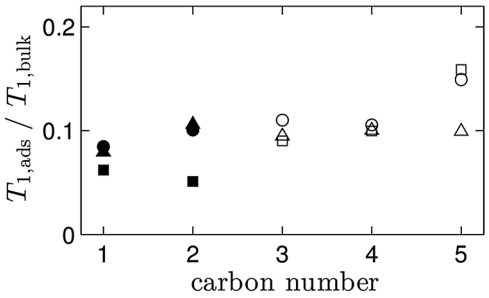

Fig. 9 The ratio of surface to bulk relaxation times $T_{1,ads}/T_{1,bulk}$ for the individual carbon atoms in 1-pentene co-adsorbed with CO on θ-Al_2O_3. Data are shown for case (i) adsorption of 0.5 ML 1-pentene followed by 0.5 ML CO (circles) and (ii) adsorption of 0.5 ML CO followed by 0.5 ML 1-pentene (triangles). For case (iii), adsorption of 0.5 ML 1-pentene only (squares), data are repeated from Fig. 6. Solid symbols represent olefinic carbons and open symbols represent aliphatic carbons.

and isobutene,[29,38] and conversion between *n*-pentene isomers,[39] has been reported with alumina as the catalyst.

The $T_{1,ads}/T_{1,bulk}$ ratios of the carbon atoms in *trans*-2-pentene show a stronger interaction for the olefinic carbons than the aliphatic carbons, as expected. In particular, C3 shows the strongest interaction. The interaction through the double-bond is notably stronger than in the case of *trans*-2-pentene adsorbed as a single component, see Fig. 2(d).

3.3 Conformation of hydrocarbons co-adsorbed on surfaces

3.3.1 Co-adsorption of 1-pentene and CO. Results from the co-adsorption of 0.9 ML CO with 0.5 ML 1-pentene are shown in Fig. 9. The $T_{1,ads}/T_{1,bulk}$ ratios are shown for three cases: (i) 1-pentene adsorbed first, followed by CO; (ii) CO adsorbed first, followed by 1-pentene; (iii) 0.5 ML of 1-pentene only for comparison. The most notable observation is that in both co-adsorption experiments the effect of the presence of CO is to weaken the interaction strength of the olefinic carbons C1 and C2 with the surface; the effect is greater for the C2 carbon than for the C1. As has already been noted, CO is co-adsorbed with unsaturated hydrocarbons in the industrial process of acetylene selective semi-hydrogenation to ethylene. One of the effects of CO in this process is to weaken the interaction of the alkene with the Pd-based active site on the catalyst thereby limiting further hydrogenation of ethylene to the undesired total hydrogenation product: ethane.[19] Although our data were acquired in the absence of a metal catalyst, we note that CO, when physisorbed on the surface, weakens the alkene–alumina interaction.

Further comparison with the data for 0.5 ML and 1 ML 1-pentene (Fig. 6) suggest that pre-adsorption of pentene followed by adsorption of CO causes the adsorption interaction of 1-pentene to be very similar to the adsorption of single component 1-pentene at 1 ML on θ-Al_2O_3, albeit with a slightly lower interaction of the C5 carbon with the surface than in the co-adsorbed case. However, we may deduce that the conformation of 1-pentene during adsorption remains the same, with lateral interactions reducing the interaction of the C1 and C2 with the surface. In contrast, when CO is pre-adsorbed, whilst the behaviour with respect to the C1–C4 carbons is the same as when 1-pentene is pre-adsorbed, the C5 carbon appears to be held more closely to the surface. The sample was remade twice and the experiment repeated to confirm the validity of this measurement and it was found that the value of $T_{1,ads}/T_{1,bulk}$ for the C5 carbon was reproducible to within experimental error. These data suggest that when CO is pre-adsorbed, the alkyl chain of 1-pentene is more restricted, perhaps by stronger lateral interactions with the adsorbed CO.

3.3.2 Co-adsorption of 1-pentene and 2-butyne. An alkyne and alkene were co-adsorbed on θ-Al_2O_3 to study the competitive adsorption of triple and double bonds. $T_{1,ads}/T_{1,bulk}$ ratios are shown in Fig. 10 for three cases: (i) 1-pentene adsorbed first, followed by 2-butyne; (ii) 2-butyne adsorbed first, followed by 1-pentene; (iii) 0.5 ML of 1-pentene only for comparison. The $T_{1,ads}/T_{1,bulk}$ ratios of the alkyne are consistently lower than for the alkene. Therefore, adsorption of the alkyne is favoured, in agreement with the single-component adsorption studies in Section 3.1.1. In Fig. 10, the olefinic carbons of 1-pentene exhibit average $T_{1,ads}/T_{1,bulk}$ ratios of 0.061 in case (i) and 0.071 in case (ii). An average $T_{1,ads}/T_{1,bulk}$ ratio of 0.056 was obtained in case (iii). Therefore, the double bond interaction with the alumina surface is weakened by the presence of

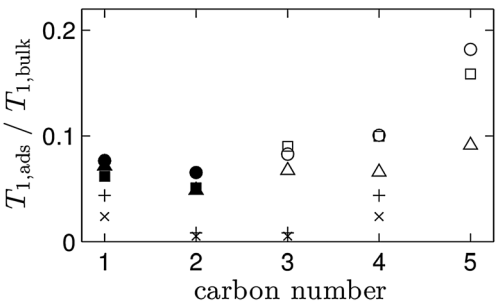

Fig. 10 The ratio of surface to bulk relaxation times $T_{1,ads}/T_{1,bulk}$ for the individual carbon atoms in 1-pentene co-adsorbed with 2-butyne on θ-Al_2O_3. Data are shown for case (i) adsorption of 0.5 ML 1-pentene (triangles) followed by 0.5 ML 2-butyne (×) and (ii) adsorption of 0.5 ML 2-butyne (+) followed by 0.5 ML 1-pentene (circles). For case (iii), adsorption of 0.5 ML 1-pentene only (squares), data are repeated from Fig. 6. Solid symbols represent olefinic carbons and open symbols represent aliphatic carbons in 1-pentene.

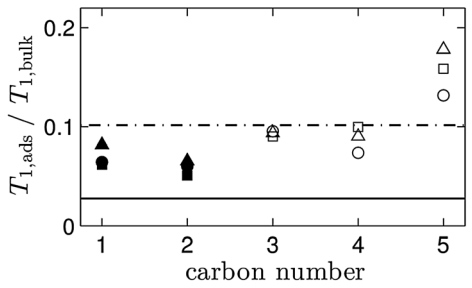

Fig. 11 The ratio of surface to bulk relaxation times $T_{1,ads}/T_{1,bulk}$ for the individual carbon atoms in 1-pentene co-adsorbed with benzene and cyclohexane on θ-Al_2O_3. Data are shown for adsorption of 0.5 ML 1-pentene following adsorption of 0.9 ML cyclohexane (circles), and adsorption of 0.5 ML 1-pentene following adsorption of 0.9 ML benzene (triangles). For comparison, data for the adsorption of 0.5 ML 1-pentene only (squares) are repeated from Fig. 6. Solid symbols represent olefinic carbons and open symbols represent aliphatic carbons. The single $T_{1,ads}/T_{1,bulk}$ ratios for benzene (solid line) and cyclohexane (dash-dot line) are included.

the alkyne. It is also noted that in the case of 1-pentene pre-adsorption, the interaction of C5 with the surface is again reduced significantly compared to that observed for pure 1-pentene adsorption and when 2-butyne is pre-adsorbed.

The aliphatic carbons of 1-pentene are less mobile in case (i) than in case (ii) and (iii) due to lateral molecule–molecule interactions with excess 2-butyne. Similarly, in case (ii), C1 and C4 of 2-butyne present higher $T_{1,ads}/T_{1,bulk}$ ratios (weaker interaction) than in case (i), most likely due to higher 2-butyne effective adsorption coverage and possibly due to interactions with adsorbed 1-pentene.

3.3.3 Co-adsorption of 1-pentene and cyclic hydrocarbons. Finally, the adsorption of 0.5 ML of 1-pentene on θ-Al_2O_3 is investigated after pre-adsorption of (i) 0.9 ML of cyclohexane and (ii) 0.9 ML of benzene. Cyclohexane and benzene are used here to model coke deposition at different stages of catalyst deactivation. Fig. 11 shows the carbon-specific $T_{1,ads}/T_{1,bulk}$ ratios for 1-pentene, as well as a single $T_{1,ads}/T_{1,bulk}$ value for cyclohexane and benzene where the individual carbons are indistinguishable. The $T_{1,ads}/T_{1,bulk}$ ratio for benzene (solid line) is always lower than for carbons C1 and C2 of 1-pentene. Conversely, the $T_{1,ads}/T_{1,bulk}$ ratio for cyclohexane (dash-dot line) is higher than carbons C1 and C2 of 1-pentene. These results are in agreement with previous literature on coke formation and catalyst deactivation.[40] The formation of graphitic deposits prevents adsorption and subsequent reaction of the desired product. The average $T_{1,ads}/T_{1,bulk}$ ratio of the olefinic carbons is 0.063 in case (i) and 0.074 in case (ii). These values are comparable to those obtained for single-component 1-pentene adsorbed on θ-Al_2O_3. Overall, a weakening of the double-bond interaction with the alumina surface is inferred in the presence of coke, with the pre-adsorption of benzene, representing hard coke, causing the greater reduction in the interaction of 1-pentene with the surface.

4 Conclusions

We have reported the application of chemical shift resolved ^{13}C NMR T_1 relaxation time analysis to the determination of adsorbate interaction with alumina surfaces. The method allows the relative strength of surface interaction of individual carbon atoms to be inferred unambiguously. The adsorbents used in this study are in a physical form of relevance to industrial processes such as gas separations and gas-phase heterogeneous catalysis. These factors comprise significant advances over existing techniques for probing surface adsorption, notably in the study of co-adsorbed species. Therefore, this NMR method represents an important addition to the toolbox available for studying adsorption, co-adsorption, and molecular conformation on catalyst surfaces.

For the specific molecules studied, it was observed that all the unsaturated molecules bonded weakly to the porous alumina surface. An acetylenic functionality was observed to have a stronger interaction than olefinic functionalities. Adsorption was confirmed to be more favourable over θ-Al_2O_3 than over γ-Al_2O_3, as expected from the higher surface acidity of the θ-Al_2O_3. Studies of adsorption as a function of surface coverage demonstrated the average interaction strength was greater at lower coverage, indicating molecules adsorb preferentially on the strongest adsorption sites. In addition to information on atom-specific, adsorbate–adsorbent interaction strengths, the molecular conformations of the adsorbates were inferred. Finally, the co-adsorption studies demonstrate the application of the ^{13}C NMR $T_{1,ads}/T_{1,bulk}$ relaxation time measurement to gain insight into how the presence of one species modifies the adsorption behaviour of a second species. As long as distinct spectral resonances can be identified, more complex mixtures can be studied. In ongoing work, this approach is being used to both understand reaction pathways in heterogeneous catalysis and aid the selection of materials for specific catalytic processes.

Acknowledgements

This work was supported through the CASTech project (EPSRC grant EP/G011397/1) and the ATHENA project (EPSRC grant GR/R47523/01) and by Johnson Matthey plc. For additional financial support, P. A. Vecino acknowledges a Cambridge European Trust Santander Scholarship. The authors thank Tegan Roberts, Andy Sederman, Mick Mantle, and Andy York for helpful discussions.

Notes and references

1 T. Mallat, E. Orglmeister and A. Baiker, *Chem. Rev.*, 2007, **107**, 4863.
2 M. J. Gladys, A. V. Stevens, N. R. Scott, G. Jones, D. Batchelor and G. Held, *J. Phys. Chem. C*, 2007, **111**, 8331.
3 C. L. A. Lamont, M. Borbach, R. Martin, P. Gardner, T. S. Jones, H. Conrad and A. M. Bradshaw, *Surf. Sci.*, 1997, **374**, 215; M. Yang, K. C. Chou and G. A. Somorjai, *J. Phys. Chem. B*, 2004, **108**, 14766.
4 A. M. Buchbinder, E. Weitz and F. M. Geiger, *J. Phys. Chem. C*, 2010, **114**, 554.

5 M. V. Popova, Y. S. Tchernyshev and D. Michel, *Colloid Polym. Sci.*, 2006, **285**, 359.
6 C. Sievers, A. Onda, R. Olindo and J. A. Lercher, *J. Phys. Chem. C*, 2007, **111**, 5454.
7 D. Rouabah, R. Benslama and J. Fraissard, *Chem. Phys. Lett.*, 1991, **179**, 218; M. Polisset and J. Fraissard, *Colloids Surf., A*, 1993, **72**, 197.
8 V. L. Budarin, J. H. Clark, F. E. I. Deswarte, K. T. Mueller and S. J. Tavener, *Phys. Chem. Chem. Phys.*, 2007, **9**, 2274; V. L. Budarin, J. H. Clark, S. E. Hale, S. J. Tavener, K. T. Mueller and N. M. Washton, *Langmuir*, 2007, **23**, 5412.
9 X. Q. Xie, S. V. Ranade and A. T. DiBenedetto, *Polymer*, 1999, **40**, 6297.
10 D. Denney, V. M. Mastikhin, S. Namba and J. Turkevich, *J. Phys. Chem.*, 1978, **82**, 1752.
11 R. Kimmich, *NMR – Tomography, Diffusometry, Relaxometry*, Springer-Verlag, Berlin, 1997.
12 G. Liu, Y. Li and J. Jonas, *J. Chem. Phys.*, 1991, **95**, 6892.
13 M. Monduzzi, R. Monaci and V. Solinas, *J. Colloid Interface Sci.*, 1987, **120**, 8.
14 D. W. Weber, J. Mitchell, J. McGregor and L. F. Gladden, *J. Phys. Chem. C*, 2009, **113**, 6610.
15 J. Mitchell, T. C. Chandrasekera, M. L. Johns and L. F. Gladden, *Phys. Rev. E: Stat., Nonlinear, Soft Matter Phys.*, 2010, **81**, 026101.
16 K. E. Washburn, C. D. Eccles and P. T. Callaghan, *J. Magn. Reson.*, 2008, **194**, 33.
17 A. Corado, A. Kiss, H. Knoezinger and H. D. Mueller, *J. Catal.*, 1975, **37**, 68; M. Guisnet, J. L. Lemberton, G. Perot and R. Maurel, *J. Catal.*, 1977, **48**, 166; Y. Hong, F. R. Chen and J. J. Fripiat, *Catal. Lett.*, 1993, **17**, 187; Y. Amenomiya, J. H. B. Chenier and R. J. Cvetanovic, *J. Catal.*, 1967, **9**, 28.
18 N. S. Gnep and J. Y. Doyement, *Appl. Catal.*, 1988, **43**, 155.
19 N. López, B. Bridier and J. Pérez-Ramírez, *J. Phys. Chem. C*, 2008, **112**, 9346; Y. H. Park and G. L. Price, *Ind. Eng. Chem. Res.*, 1991, **30**, 1693.
20 C. E. Webster, R. S. Drago and M. C. Zerner, *J. Am. Chem. Soc.*, 1998, **120**, 5509.
21 J. Keeler, *Understanding NMR Spectroscopy*, John Wiley & Sons Ltd, Chichester, 2005; D. Weber, A. J. Sederman, M. D. Mantle, J. Mitchell and L. F. Gladden, *Phys. Chem. Chem. Phys.*, 2010, **12**, 2619.
22 C. De la Cruz and N. Sheppard, *J. Mol. Struct.*, 1991, **247**, 25; G. Shahid and N. Sheppard, *Can. J. Chem.*, 1991, **69**, 1812.
23 G. Shahid and N. Sheppard, *J. Chem. Soc., Faraday Trans.*, 1994, **90**, 507.
24 J. McGregor and L. F. Gladden, *Appl. Catal., A*, 2008, **345**, 51; Z. Dobrovolná, P. Kacer and L. Cervený, *J. Mol. Catal. A: Chem.*, 1998, **130**, 279; A. S. Canning, S. D. Jackson, A. Monaghan and T. Wright, *Catal. Today*, 2006, **116**, 22.
25 R. H. Meinhold, R. C. T. Slade and R. H. Newman, *Appl. Magn. Reson.*, 1993, **4**, 121; C.-F. Mao and M. A. Vannice, *Appl. Catal., A*, 1994, **111**, 151.
26 Y. R. Zhou, W. P. Zhu, F. D. Liu, J. B. Wang and S. X. Yang, *Acta Chim. Sin.*, 2006, **64**, 889.
27 N. R. Avery and N. Sheppard, *Proc. R. Soc. London, Ser. A*, 1986, **405**, 1; N. R. Avery and N. Sheppard, *Surf. Sci.*, 1986, **169**, L367; B. A. Morrow and N. Sheppard, *Proc. R. Soc. London, Ser. A*, 1969, **311**, 415.
28 G. Busca, E. Finocchio, V. Lorenzelli, M. Trombetta and S. A. Rossini, *J. Chem. Soc., Faraday Trans.*, 1996, **92**, 4687.
29 M. Trombetta, G. Busca, S. A. Rossini, V. Piccoli and U. Cornaro, *J. Catal.*, 1997, **168**, 334.
30 M. Saeys, M. F. Reyniers, M. Neurock and G. B. Marin, *Surf. Sci.*, 2006, **600**, 3121; C. Xu and B. E. Koel, *Surf. Sci.*, 1994, **304**, 249; F. C. Henn, A. L. Diaz, M. E. Bussell, M. B. Hugenschmidt, M. E. Domagala and C. T. Campbell, *J. Phys. Chem.*, 1992, **96**, 5965.
31 A. A. Gabrienko, S. S. Arzumanov, D. Freude and A. G. Stepanov, *J. Phys. Chem. C*, 2010, **114**, 12681; A. G. Stepanov, S. S. Arzumanov, M. V. Luzgin, H. Ernst and D. Freude, *J. Catal.*, 2005, **229**, 243.
32 J. Shen, R. D. Cortright, Y. Chen and J. A. Dumesic, *J. Phys. Chem.*, 1994, **98**, 8067.
33 M. J. Calhorda, P. E. M. Lopes and C. M. Friend, *J. Mol. Catal. A: Chem.*, 1995, **97**, 157; R. J. Koestner, M. A. Van Hove and G. A. Somorjai, *J. Phys. Chem.*, 1983, **87**, 203; R. F. Lin, R. J. Koestner, M. A. Van Hove and G. A. Somorjai, *Surf. Sci.*, 1983, **134**, 161.
34 B. P. Miller, O. J. Furlong and W. T. Tysoe, *Surf. Sci.*, 2013, **616**, 143; J. Pawela-Crew and R. J. Madix, *Surf. Sci.*, 1995, **339**, 8.
35 G. Aguilar-Armenta, M. E. Patiño-Iglesias, J. Jiménez-Jiménez, E. Rodríguez-Castellón and A. Jiménez-López, *Langmuir*, 2006, **22**, 1260.
36 X. Liu and R. E. Truitt, *J. Am. Chem. Soc.*, 1997, **119**, 9857; C. Morterra and G. Magnacca, *Catal. Today*, 1996, **27**, 497.
37 M. Digne, P. Sautet, P. Raybaud, P. Euzen and H. Toulhoat, *J. Catal.*, 2002, **211**, 1.
38 Z. X. Cheng and V. Ponec, *J. Catal.*, 1995, **148**, 607.
39 A. G. Oblad, J. U. Messenger and H. T. Brown, *Ind. Eng. Chem.*, 1947, **39**, 1462.
40 D. Chen, H. P. Rebo, A. Grønvold, K. Moljord and A. Holmen, *Microporous Mesoporous Mater.*, 2000, **35–36**, 121; J. McGregor, Z. Huang, E. P. J. Parrott, J. A. Zeitler, K. L. Nguyen, J. M. Rawson, A. Carley, T. W. Hansen, J. P. Tessonnier, D. S. Su, D. Teschner, E. M. Vass, A. Knop-Gericke, R. Schlögl and L. F. Gladden, *J. Catal.*, 2010, **269**, 329.